

Is Active IRS Useful for mmWave Wireless Networks or Not?

Jalal Jalali[†], Ata Khalili[‡], Atefeh Rezaei^{*}, and Jeroen Famaey[†]

[†]IDLab, University of Antwerp - imec, Sint-Pietersvliet 7, 2000 Antwerp, Belgium

^{*}Department of Electrical and Computer Engineering, Tarbiat Modares University, Tehran 14115-111, Iran

[‡]Institute for Digital Communications, Friedrich-Alexander-University Erlangen-Nurnberg, Erlangen, Germany

Email: jalal.jalali@uantwerpen.be

Abstract—Recently, intelligent reflecting surfaces (IRSs) have been proposed to enhance the system performance of several applications via smartly reconfiguring signal propagation. Precisely, as low-cost passive devices, IRSs control the scattering, refraction, and reflection characteristics of the radio waves to suppress the interference at one or more desired receivers. In this paper, it is assumed that an active IRS-assisted multiple-input single-output (MISO) system aids a millimeter-wave (mmWave) wireless network. So, the signal sent from the access point (AP) could be reflected by the IRS and simultaneously be received by the user. To achieve the full gain of IRS-assisted wireless networks, not only the phase shift at the IRS should be optimized, but the amplitude variation with low-cost hardware at the IRS should also be exploited. Thus, in this paper, we formulate the system sum rate maximization problem to optimize both the active and passive beamformer at the AP and the IRS, considering amplitude control at the IRS from the limited available power with low-cost hardware. To do so, two low-complexity algorithms are developed. In particular, the first subproblem is solved based on the weighted minimum square error (WMMSE) to optimize the beamforming at the AP. The second sub-problem is solved via successive convex approximation. Numerical results show that active IRS is beneficial and achieves better gains as compared to passive IRS.

Index Terms: Intelligent reflecting surface (IRS), millimeter-wave (mmWave), weighted minimum mean square error (WMMSE), successive convex approximation (SCA).

I. INTRODUCTION

In order to accommodate the need for high data rate multi-media access, the capacity of current wireless networks should significantly expand by a variety of wireless technologies and topologies. As explored in the last decade, ultra-dense network massive multiple-input multiple-output (MIMO), as well as using new techniques such as the millimeter-wave (mmWave) bands, could help increase the need for capacity [1]. However, designing access points with more antenna elements and utilizing radio frequency (RF) chains at extremely high frequencies in practical mmWave systems certainly affect the hardware expenditure and the network energy consumption of the systems. Hence, new approaches that cover both spectral- and energy-efficiency aims are required for the deployment and evolution of sustainable wireless networks in the future [2], [3]. In order to achieve the above aims, intelligent re-

flecting surfaces (IRS) are a vital enabler for smart radio environments. In this recent emerging hardware technology, several artificial passive elements with low-cost printed dipoles reflect the incident radio frequency waves in a certain direction with low power consumption. These elements are attached to a smart controller to change the reflected signal propagation. Clearly, due to using passive reflection beamforming, an IRS consumes much less power than what could be perpetrated by a traditional amplify-and-forward (AF) relay, and also no additional thermal noise is added while reflecting [4], [5].

Most contemporary existent works on IRS communication systems have focused on optimizing the IRS parameters for outdoor communication systems [6]–[8]. For example, in [6], an IRS-assisted single-cell multi-user multiple-input single-output (MISO) system was assumed, and the values of the induced phases for passive and active beamformer were optimized to enlarge the aggregate received signal power at the single-antenna users. The works in [7], [8] maximized the energy- and spectral-efficiency of an IRS-aided multi-user MISO network via designing a transmit power allocation policy at the access point (AP) and finding the IRS phase-shifts when zero-forcing precoding applied in the digital domain. Although a variety of papers reported on IRS-based networks [9], [10], a limited number of works consider controlling the reflection amplitudes in the IRS system [3], [11]. The authors in [3], [11] studied the efficiency of considering amplitude variation in a network with imperfect channel state information (CSI). They employed a penalized Dinkelbach and block successive upper-bound minimization algorithms to optimize reflection coefficients so as to maximize the attainable data rate. As a result of controlling the reflection amplitudes, additional performance gains are achieved compared with the full reflection/phase-shift control. Moreover, answering whether to go with passive or active IRS deployment in the next generation of wireless communication networks led to recent attraction in the field [12]–[16]. The authors in [12] optimized IRS placement to maximize the data rate of a single-user single-input single-output (SISO) system with an active or passive IRS and a single-antenna AP. To tolerate multiplicative fading in the sixth generation (6G) and as a true 6G-enabler, active IRS was recommended in [13]. The authors extensively investigated active IRSs and compared them with conventional

This work was supported by the CHIST-ERA grant SAMBAS (CHIST-ERA-20-SICT-003), with funding from FWO, ANR, NKFIH, and UKRI.

passive IRSs to find the performance bottleneck. An IRS-aided multi-user MISO downlink network was studied in [14] to maximize the sum data rate of users with different IRSs types in 6G. A practical active IRS design was studied in [15], where the outage probability and the secrecy outage probability were optimized for a SISO network with full CSI knowledge. Finally, authors in [16] explored a resource allocation design problem of minimizing AP's transmit power for an active IRS-enabled communication network, where the active IRSs can boost the reflected signal by using a supplemental power source.

Additionally, millimeter wave (mmWave) is a promising solution to provide higher throughput. However, this technology introduces some drawbacks to wireless networks due to having a short wavelength, such as reduced signal propagation due to absorption by obstacles. Therefore, IRS could help the network to sweeten the performance of the mmWave communication network [17]. Besides, combining these technologies could result in another problem due to inefficient use of resources [18]. Using IRS has some advantages and disadvantages in the network. For instance, although it could increase the received signal at some users, it also can increase the destructive interference in some users' receivers. We aim to address these shortcomings by controlling amplitude. The aim is to assess the performance gain via controlling the amplitude of the IRS as compared to conventional schemes in which the full reflection is exploited. To this end, we design a new optimization algorithm to maximize the network's data rate based on a mmWave channel model. In our proposed system, a weighted minimum mean square error (WMMSE) is utilized for optimization with respect to the transmit beamforming when the IRS optimization is fixed. And then, successive convex approximation (SCA) is used to optimize the amplitude and phase shift of the IRS elements when transmit beamforming is assumed given. Our simulation results reveal that exploiting the amplitude control is a promising solution to fully exploit the potential of IRS-assisted wireless systems, especially in the mmWave wireless networks.

Notations: Throughout this paper, the following notations are used. The capital bold face letters are used to denote matrices while using the small bold and small normal face to denote vectors and scalars, respectively. \mathbf{I} represents an identity matrix, $\mathbb{C}^{x \times y}$ is a $x \times y$ complex-valued matrix. The superscript $(\cdot)^H$ is the conjugate transpose of a matrix, and transpose of a matrix is expressed as $(\cdot)^T$. The notations $\mathbb{E}[\cdot]$, $\text{tr}(\cdot)$, and $\text{diag}(\cdot)$ are used to denote the statistical expectation, trace and diagonalization operator, respectively. $\nabla f(\cdot)$ reads as the gradient of the function $f(\cdot)$ and $\frac{\partial f(a)}{\partial g}$ is the first derivative of f with respect to g at $g = a$. $\|\mathbf{x}\|$ is the 2-norm of vector \mathbf{x} . $\mathcal{CN}(\boldsymbol{\mu}, \boldsymbol{\Sigma})$ gives the distribution of a circularly symmetric complex Gaussian (CSCG) random vector with the mean $\boldsymbol{\mu}$ and covariance matrix $\boldsymbol{\Sigma}$, where \sim means "with the distribution of." $\ln(\cdot)$ represents the natural logarithm of its

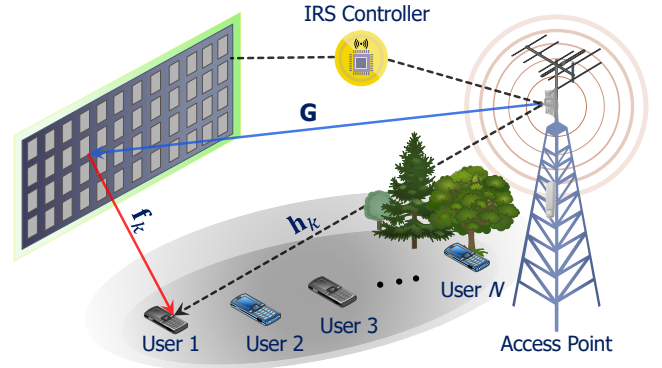


Figure 1: An IRS-assisted multi-user MISO mmWave wireless communication system.

argument, and $\Re\{\cdot\}$ signifies the real part of the argument.

II. SYSTEM MODEL

In this section, we describe the system model for the IRS-aided MISO multi-user network where an AP with N_t -antennae serves K single-antenna mobile users in downlink communication, where the set of k users is represented by $\mathcal{K} = \{1, \dots, K\}$. As shown in Fig. 1, it is considered that this communication takes place with the help of an active IRS consisting of M passive elements that act as phase shifters, deployed, for example, on a building facade in the AP's line-of-sight (LoS). We note that the set of m passive elements is shown as $\mathcal{M} = \{1, \dots, M\}$. The IRS, as a configurable and programmable device, alters its operation mode between the reflection and no-reflection modes for the downlink transmission and channel estimation phases, respectively. Moreover, it is supposed that a flat-fading channel model and perfect channel state information (CSI) knowledge are available at the AP and also IRS. We emphasize that the IRS is active so that it can adjust its phase and reflect amplitude jointly. In this system, we denote the AP to the IRS channel matrix by $\mathbf{G} \in \mathbb{C}^{M \times N_t}$. The reflecting channel vector from the IRS to user k is denoted by $\mathbf{f}_k \in \mathbb{C}^{M \times 1}$, while the direct channel vector between the AP and user k is $\mathbf{g}_k^H \in \mathbb{C}^{N_t \times 1}$. Let $\boldsymbol{\Theta} = \text{diag}(\theta_1, \theta_2, \dots, \theta_M)$ be the diagonal phase shift matrix for the IRS where $\theta_m = e^{j\varphi_m}$ is the phase shift of the m -th reflecting element of the IRS, where $\varphi_m \in [0, 2\pi)$ with j representing the imaginary unit. Let's also define, $\mathbf{A} = \text{diag}(\alpha_1, \alpha_2, \dots, \alpha_M)$ be the amplitude control matrix for the IRS, where the amplitudes span between zero and the maximum allowable budget, α_{\max} , i.e., $\alpha_n \in [0, \alpha_{\max}]$. Despite the works in [6], [18] that considered IRS with full reflection, i.e., $\alpha_m = 1 \forall m$, in this paper, we evaluate amplitude and phase shift control jointly at the IRS in order to achieve the full gain of the IRS.

A. Channel Model

Full CSI knowledge helps disclose the upper bound of the performance gain [9]. The mmWave real-valued channel matrix \mathbf{G} follows the Saleh-Valenzuela model [19] and is given by:

$$\mathbf{G} = \sqrt{N_t \times M} \sum_{i=0}^{\Delta} \gamma_i \zeta_t \zeta_r \alpha_M(\varphi_i) \alpha_{N_t}(\theta_i), \quad (1)$$

where, Δ , represents the number of paths including the line-of-sight and none-line-of-sight paths. ζ_t and ζ_r are the transmit and receive antenna gains, respectively. Additionally, γ_i stands for complex gain of i -th path, φ_i , and θ_i are the angles of arrival and the angle of departure for the i -th path, respectively [19]. Also, the array response function of the IRS can be expressed as:

$$\alpha_M(\varphi) = \frac{1}{\sqrt{M}} \left[e^{j2\pi(d/\lambda)\sin(\varphi)} \right], \quad (2)$$

$$\alpha_{N_t}(\theta) = \frac{1}{\sqrt{N_t}} \left[e^{j2\pi(d/\lambda)\sin(\theta)} \right], \quad (3)$$

where λ and d denote the mmWave wavelength and the antenna spacing, respectively. Therefore, the channel gain from the IRS to the user k is:

$$\mathbf{f}_k = \sqrt{M} \zeta_t \zeta_r \gamma_i \alpha_M(\varphi). \quad (4)$$

Since mmWave links are highly susceptible to blockages, the direct channel gain between the AP and each user is really weak. In such a system model, the received signals at the mobile user k is then written as:

$$y_k = (\mathbf{g}_k^H + \mathbf{f}_k^H \mathbf{A} \Theta \mathbf{G}) x + \mathbf{f}_k^H \mathbf{A} \Theta n_d + n_k, \quad (5)$$

where $x = \sum_{k=1}^K \mathbf{w}_k s_k$ is the transmitted signal at the AP in which s_k is the transmit data symbol to the k -th user and $\mathbf{w}_k \in \mathbb{C}^{N_t \times 1}$ is the corresponding transmit beamforming vector. We also note that the transmit data vector for K users can be represented as $\mathbf{s} = [s_1, \dots, s_K]$, where $\mathbb{E}[\mathbf{s}\mathbf{s}^H] = \mathbf{I}$. n_d is the dynamic noise that originates from the contributing input noise and the intrinsic device noise of the active RIS, while n_k is the static noise [20]. n_d and n_k represent the additive complex Gaussian (AWGN) terms with a circularly symmetric Gaussian distribution, i.e., $n_d \sim \mathcal{CN}(0, \sigma_d^2)$ and $n_k \sim \mathcal{CN}(0, \sigma_k^2)$, respectively. Accordingly, the received signal-to-interference-plus-noise ratio (SINR) at the receiver k can be expressed as:

$$\gamma_k = \frac{|\mathbf{f}_k^H \mathbf{A} \Theta \mathbf{G} \mathbf{w}_k|^2}{\sum_{i=1, i \neq k}^K |\mathbf{f}_k^H \mathbf{A} \Theta \mathbf{G} \mathbf{w}_i|^2 + \sigma_d^2 |\mathbf{f}_k^H \mathbf{A} \Theta|^2 + \sigma_k^2}, \quad \forall k \in \mathcal{K}. \quad (6)$$

III. PROBLEM FORMULATION

In this section, we maximize the total sum data rate by optimizing the corresponding transmit beamforming matrix $\mathbf{W} = [\mathbf{w}_1, \dots, \mathbf{w}_K] \in \mathbb{C}^{N_t \times K}$ at the AP and reflection coefficients at the IRS. The associate optimization problem is

formulated as:

$$\mathbf{P}_1 : \max_{\mathbf{W}, \theta_m, \alpha_m} \sum_{k=1}^K R_k \quad (7a)$$

$$\text{s.t.} : \sum_{k=1}^K \|\mathbf{w}_k\|^2 \leq P_{\max}, \quad (7b)$$

$$0 \leq \theta_m < 2\pi, \quad \forall m \in \mathcal{M}, \quad (7c)$$

$$0 \leq \alpha_m \leq \alpha_{\max}, \quad \forall m \in \mathcal{M}, \quad (7d)$$

$$\sum_{k=1}^K |\mathbf{A} \Theta \mathbf{G} \mathbf{w}_k|^2 + \sigma_d^2 |\mathbf{A} \Theta|^2 \leq P_A, \quad (7e)$$

where $R_k = \ln(1 + \gamma_k)$. Noting that the objective function of \mathbf{P}_1 and the constraints are not convex, hence, the optimization problem \mathbf{P}_1 is a non-convex optimization problem. In \mathbf{P}_1 , constraint (7b) means there is a limit on the total transmit power of the AP, that is the maximum transmit power P_{\max} . Also, the constraints in (7c) and (7d) define that each reflecting element can be adjusted according to its phase and reflecting amplitude coefficients, respectively. This brings an additional degree of freedom into our problem that enhances the performance gain of the wireless network. Finally, the constraint (7e) implies that the amplification power of the active IRS must not exceed the maximum power allowance P_A .

Solving the optimization problem \mathbf{P}_1 is challenging due to the non-convex functions in the objection and constraints. We propose an iterative approach for designing parameters of this optimization in which power allocation and phase-shift are iteratively solved. In particular, for given reflection coefficient Θ and amplitude control \mathbf{A} , we find the optimum transmit beamforming \mathbf{W} , and then solve for \mathbf{W} when Θ and \mathbf{A} are fixed. This iterative process continues until it converges to the optimum value of the objective. In the rest of this section, we describe this iterative algorithm.

A. Optimization with respect to the Transmit Beamforming

For given reflection coefficient Θ and amplitude control coefficient \mathbf{A} , the optimization problem \mathbf{P}_1 is reduced to:

$$\mathbf{P}_2 : \max_{\mathbf{W}} \sum_{k=1}^K R_k \quad (8a)$$

$$\text{s.t.} : \sum_{k=1}^K \|\mathbf{w}_k\|^2 \leq P_{\max}, \quad (8b)$$

$$\sum_{k=1}^K |\mathbf{A} \Theta \mathbf{G} \mathbf{w}_k|^2 + \sigma_d^2 |\mathbf{A} \Theta|^2 \leq P_A, \quad (8c)$$

where $R_k = \ln(1 + \gamma_k)$ with the SINR, γ_k , given by:

$$\gamma_k = \frac{|\mathbf{h}_k^H \mathbf{w}_k|^2}{\sum_{i=1, i \neq k}^K |\mathbf{h}_k^H \mathbf{w}_i|^2 + \sigma_d^2 |\mathbf{f}_k^H \mathbf{A} \Theta|^2 + \sigma_k^2}, \quad \forall k \in \mathcal{K}, \quad (9)$$

in which $\mathbf{h}_k^H = \mathbf{g}_k^H + \mathbf{f}_k^H \mathbf{A} \Theta \mathbf{G}$ denotes the combined channel from the AP to the k -th user. In order to solve the above optimization problem, we introduce the use of WMMSE algorithm. The main idea of this algorithm is to

reformulate the weighted sum rate problem into its equivalent WMMSE problem formulation and solve it via the alternating optimization method. To do so, we assume the signal s_k is decoded by using the equalizer u_k , so the estimated signal at user k is:

$$\hat{s}_k = u_k y_k, \quad \forall k \in \mathcal{K} \quad (10)$$

Under the independence assumption of s_k 's and n_k 's, the mean square errors (MSEs), which is defined by $e_k = \mathbb{E} \left[|\hat{s}_k - s_k|^2 \right]$, can be calculated as:

$$e_k = |u_k|^2 B_k - 2\Re \{ u_k \mathbf{h}_k^H \mathbf{w}_k \} + 1, \quad (11)$$

where $B_k = |\mathbf{h}_k^H \mathbf{w}_k|^2 + \sum_{i=1}^K |\mathbf{h}_k^H \mathbf{w}_i|^2 + \sigma_d^2 |\mathbf{f}_k^H \mathbf{A} \mathbf{\Theta}|^2 + \sigma_k^2$. The optimum minimized MSEs (MMSEs) equalizer can be obtained as:

$$y_k^{\text{MMSE}} = \mathbf{w}_k^H \mathbf{h}_k B_k^{-1}, \quad (12)$$

which is calculated using $\frac{\partial e_k}{\partial y_k} = 0$ when all transmit beamformers \mathbf{W} are fixed. Accordingly, by replacing (12) into (11), the minimum mean square error (MMSE) becomes:

$$e_k^{\text{MMSE}} = \min_{u_k} e_k = B_k^{-1} \left(B_k - |\mathbf{h}_k^H \mathbf{w}_k|^2 \right), \quad (13)$$

So, the SINR of the k -th user can be expressed as $1 + \gamma_k = (e_k^{\text{MMSE}})^{-1}$ and the corresponding rate is $R_k = -\ln(e_k^{\text{MMSE}})$ [21]. The augmented weighted mean square error (WMSE) is:

$$E_k = \rho_k e_k - \ln(\rho_k), \quad (14)$$

where ρ_k is the weight associated of the MSE of the k -th user. The optimum equalizer which is the same as the MMSE equalizer can be derived by solving $\frac{\partial E_k}{\partial u_k} = 0$, and then the corresponding optimal augmented WMSE is:

$$E_k(y_k^{\text{MMSE}}) = \rho_k e_k^{\text{MMSE}} - \ln(\rho_k), \quad (15)$$

The optimal weight of the MMSE is achieved as follows:

$$\frac{\partial E_k(y_k^{\text{MMSE}})}{\partial \rho_k} = 0 \rightarrow \rho_k^* = (\ln 2 \cdot e_k^{\text{MMSE}})^{-1}, \quad (16)$$

Finally, motivated by the data rate WMMSE relationship in (16), the optimization problem P_2 is transformed into:

$$P_3 : \min_{\mathbf{W}, \boldsymbol{\rho}, \mathbf{U}} \sum_{k=1}^K [\rho_k e_k^{\text{MMSE}} - \ln(\rho_k)] \quad (17a)$$

$$\text{s.t.} : \sum_{k=1}^K \|\mathbf{w}_k\|^2 \leq P_{\max}, \quad (17b)$$

$$\sum_{k=1}^K |\mathbf{A} \mathbf{\Theta} \mathbf{G} \mathbf{w}_k|^2 + \sigma_d^2 |\mathbf{A} \mathbf{\Theta}|^2 \leq P_A, \quad (17c)$$

where $\boldsymbol{\rho} = [\rho_1, \dots, \rho_K]$ denotes the MSE weights and $\mathbf{U} = [u_1, \dots, u_K]$ represents the equalizer vectors. It can be easily shown that when we minimize P_3 with respect to $\boldsymbol{\rho}$ and \mathbf{U} , respectively, the MMSE solutions ($\boldsymbol{\rho}^{\text{MMSE}}, \mathbf{U}^{\text{MMSE}}$) including the corresponding MMSE weights and equalizers can be achieved. While fixing $\{\boldsymbol{\rho}, \mathbf{U}\}$, the optimization problem P_3 is now changed into a quadratic constrained quadratic programming (QCQP) problem at the point \mathbf{W} . Thus, a standard convex optimization package like CVX can be employed to solve the optimization problem efficiently [10], [22]–[25].

B. Optimization with respect to the IRS parameters

In this section we aim to optimize the reflection coefficients for the given beamforming. In particular, with a fixed value of \mathbf{W} , the problem P_1 is changed as follows:

$$P_4 : \max_{\theta_m, \alpha_m} \sum_{k=1}^K R_k \quad (18a)$$

$$\text{s.t.} : \sum_{k=1}^K |\mathbf{A} \mathbf{\Theta} \mathbf{G} \mathbf{w}_k|^2 + \sigma_d^2 |\mathbf{A} \mathbf{\Theta}|^2 \leq P_A \quad (18b)$$

$$0 \leq \theta_m < 2\pi, \quad \forall m \in \mathcal{M}, \quad (18c)$$

$$0 \leq \alpha_m \leq \alpha_{\max}, \quad \forall m \in \mathcal{M}, \quad (18d)$$

To simplify notation, we introduce a new matrix for the product of matrices \mathbf{A} and $\mathbf{\Theta}$. Therefore, we rewrite the product term of \mathbf{A} and $\mathbf{\Theta}$ as:

$$\Xi \triangleq \text{diag}(a_1 e^{j\theta_1}, \dots, \alpha_M e^{j\theta_M}). \quad (19)$$

We also define $\chi_m = \alpha_m e^{j\theta_m}, \forall m \in \mathcal{M}$ and $\boldsymbol{\chi} = [\chi_1, \dots, \chi_M]^T$. Consequently, we have:

$$\mathbf{f}_k^H \Xi \mathbf{G} \mathbf{w}_k \triangleq \boldsymbol{\psi}_k^H \boldsymbol{\chi}, \quad (20)$$

$$\mathbf{g}_k^H \mathbf{w}_k \triangleq \tilde{g}_{k,n}, \quad (21)$$

where $\boldsymbol{\psi}_k^H = (\text{diag}(\mathbf{f}_k^H) \mathbf{G} \mathbf{w}_k)^*$. As a result, via introducing slack variable ζ_k , the main optimization problem P_4 can be formulated as follows:

$$P_5 : \max_{\boldsymbol{\chi}, \boldsymbol{\zeta}} \sum_{k=1}^K \log_2(1 + \zeta_k) \quad (22a)$$

$$\text{s.t.} : \frac{|\boldsymbol{\psi}_k^H \boldsymbol{\chi} + \tilde{g}_k|^2}{\sum_{i \neq k} |\boldsymbol{\psi}_i^H \boldsymbol{\chi} + \tilde{g}_i|^2 + \sigma_d^2 |\boldsymbol{\chi}|^2 + \sigma_k^2} \geq \zeta_k, \quad \forall k \in \mathcal{K}, \quad (22b)$$

$$\sum_{k=1}^K |\Xi \mathbf{w}_k|^2 + \sigma_d^2 |\Xi|^2 \leq P_A, \quad (22c)$$

$$|\chi_m| \leq \alpha_m, \quad \forall m \in \mathcal{M}, \quad (22d)$$

$$(18c), (18d), \quad (22e)$$

where $\boldsymbol{\zeta} = [\zeta_1, \dots, \zeta_K]^T$. Next, we address the non-convexity of constraint (22b) based on orienting a slack variable, namely Υ_k , into the above optimization problem. Hence (22b) can be restated into the two following inequalities:

$$\sum_{i \neq k} |\boldsymbol{\psi}_i^H \boldsymbol{\chi} + \tilde{g}_i|^2 + \sigma_d^2 |\boldsymbol{\chi}|^2 + \sigma_k^2 \leq \Upsilon_k, \quad (23)$$

$$|\boldsymbol{\psi}_k^H \boldsymbol{\chi} + \tilde{g}_k|^2 \geq \Upsilon_k \zeta_k, \quad (24)$$

where $\Upsilon_k \zeta_k = \frac{1}{2}(\Upsilon_k + \zeta_k)^2 - \frac{1}{2}(\Upsilon_k^2 + \zeta_k^2)$. Note that (24) and (24) are the two new constraints to P_5 , replacing (22b). Although the (24) is a convex constraint, in contrast, the same cannot be held for (24) due to its non-convexity. In order to assemble (24) in a convex form, we adopt the SCA algorithm based on the difference of the two concave function approach

as follows [10], [23], [24]:

$$2\Re\left\{(\psi_k^H \chi^{[t']} + \tilde{g}_k)^H \psi_k^H \chi\right\} - \left|\psi_k^H \chi^{[t']} + \tilde{g}_k\right|^2 \geq \quad (25)$$

$$\frac{1}{2}(\Upsilon_k + \zeta_k)^2 - \frac{1}{2}((\Upsilon_k^2)^{[t']} + (\zeta_k^2)^{[t']})$$

$$- (\Upsilon_k)^{[t']}(\Upsilon_k - (\Upsilon_k)^{[t']}) - (\zeta_k)^{[t']}(\zeta_k - (\zeta_k)^{[t']}),$$

where $\chi^{[t']}$, $\Upsilon_k^{[t']}$, and $\zeta_k^{[t']}$ are the solution in the $[t']$ -th iteration. Now, we solve the following convex problem:

$$\begin{aligned} P_6 : \quad & \max_{\chi, \zeta, \Upsilon} \sum_{k=1}^K \log_2(1 + \zeta_k) \\ \text{s.t. : } & (18c), (18d), (22c), (22d), (23), (25). \end{aligned} \quad (26)$$

It is worth mentioning that the original problem would be ameliorated after exploiting this iterative algorithm or at least is monotonically non-decreasing after each iteration [26]. Therefore, a standard convex optimization package such as CVX could efficiently solve the optimization problem.

IV. SIMULATION RESULTS

In this section we evaluate the numerical results. We consider the AP is located at a rectangular area with a dimension of (50, 50) meters. The AP is placed at (0, 0) m, while the IRS is located at (30, 0) m and all the users are assumed to be randomly located inside the rectangular area. The path loss model is given by $35.3 + 37.6 \log_{10}(d_k)$ dB, where d_k indicates the distance between AP-user k in kilometer. As the channel characteristics, we consider that bandwidth equals 500 MHz and $\Delta = 5$. Also, $\zeta_t = 9.82$ dBm, $\zeta_r = 0$ dBm, and γ_i follows the setting described in [18]. Furthermore, the convergence tolerance is set to 10^{-2} , and a thermal noise density of -174 dBm/Hz is assumed. Also, the IRS is equipped with 60 reflecting elements and the number of users is $K = 6$. The maximum transmit power is $P_{\max} = 30$ dBm, and the maximum power allowance of the active IRS is $P_A = 13$ dBm. The static noise power at the user is set to $\sigma_k^2 = -114$ dBm, where the dynamic noise variance is $\sigma_d^2 = -110$ dBm [16], [19].

Fig. 2 shows the average sum rate versus the number of reflecting elements. As can be seen that the average sum rate increases as the number of reflecting elements increases as well. This is because increasing the number of reflecting elements provides more favorable communication to improve the performance gain of the system. However, it can be seen that there is not much performance gain in the random phase shift as compared to the scheme without IRS, which illustrates the positive impact of optimizing the phase shift at the IRS. This figure also shows that the effectiveness of active IRS as compared to the passive IRS which confirms that increasing the number of elements of the active IRS is much more efficient for improving the communication performance. In particular, in our proposed scheme not only the phase shift at the IRS is optimized but also the amplitude reflection is optimized and we can see that for a high value of

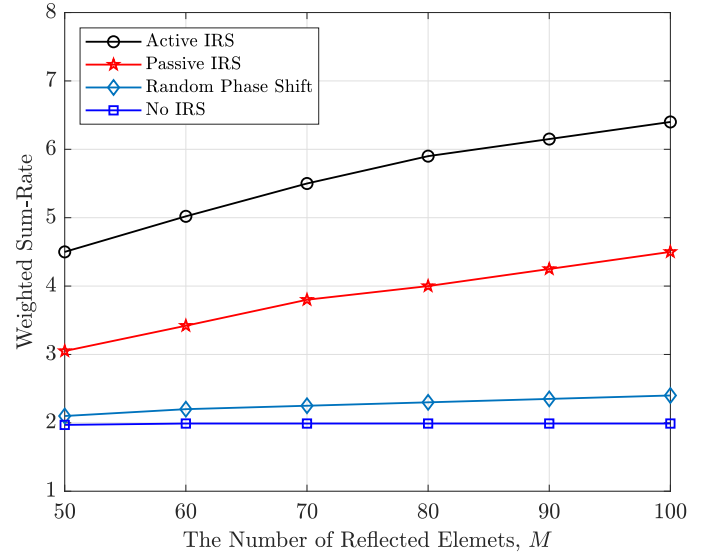


Figure 2: Average sum rate versus the number of reflecting elements.

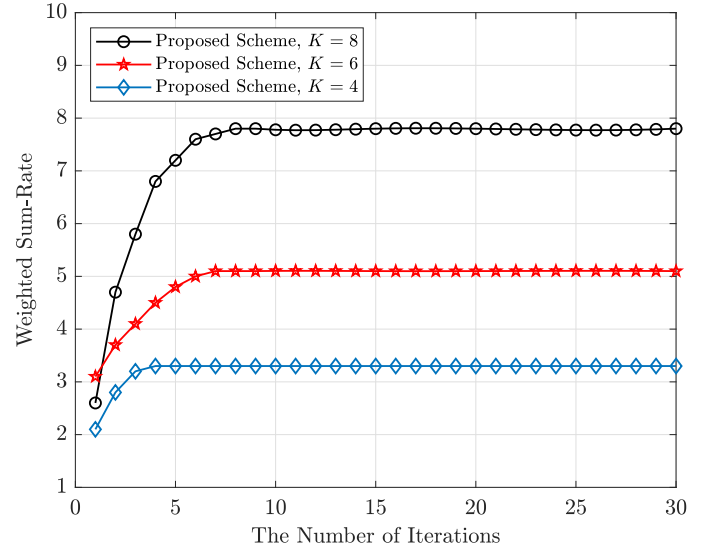


Figure 3: Average sum rate versus the number of iterations.

number of user, the performance gain that can be obtained via controlling the amplitude is more obvious. This is because the multiuser interference is more severe in the mmWave channel, which needs to be controlled via exploiting amplitude control. Besides, this results demonstrate that active IRS can overcome the “multiplicative fading” effect and attain considerable sum-rate gains.

Figure 3 plots the trend of the convergence of our proposed scheme for different numbers of users. It can be seen that our proposed algorithms converge after about 10 iterations. Besides, we can perceive that the sum rate also increases as the number of users increases as well.

V. CONCLUSION

In this paper, an optimization problem was proposed to increase the performance of mmWave wireless communication systems via designing coefficients of the IRS. Expressly, we assume an active IRS-assisted wireless MISO mmWave system to maximize the data rate of the network and design the beamformer at the AP with optimized IRS coefficients. This problem was solved iteratively in which the first sub-problem is solved via WMMSE, while the second one is solved based on the SCA approach. Simulation results unveiled the effectiveness of active IRS as compared to the passive IRS. The results, also demonstrated that the active IRS could combat the performance degradation which caused by multiplicative fading. In our future work, we will consider the effect of active IRS in the mmWave channel for the case of imperfect CSI by considering the code-book design for beamforming at the AP.

REFERENCES

- [1] F. Boccardi, R. W. Heath, A. Lozano, T. L. Marzetta, and P. Popovski, "Five disruptive technology directions for 5G," *IEEE Commun. Mag.*, vol. 52, pp. 74–80, Feb. 2014.
- [2] J. G. Andrews, S. Buzzi, W. Choi, S. V. Hanly, A. Lozano, A. C. K. Soong, and J. C. Zhang, "What will 5G be?," *IEEE J. Sel. Areas Commun.*, vol. 32, pp. 1065–1082, Jun. 2014.
- [3] M.-M. Zhao, Q. Wu, M.-J. Zhao, and R. Zhang, "IRS-aided wireless communication with imperfect CSI: Is amplitude control helpful or not?," in *Proc. IEEE GLOBECOM*, pp. 1–6, Feb. 2020.
- [4] X. Tan, Z. Sun, D. Koutsonikolas, and J. M. Jornet, "Enabling indoor mobile millimeter-wave networks based on smart reflect-arrays," in *Proc. IEEE INFOCOM*, pp. 270–278, Apr. 2018.
- [5] L. Li, T. J. Cui, W. Ji, S. Liu, J. Ding, X. Wan, Y. B. Li, M. Jiang, C.-W. Qiu, and S. Zhang, "Electromagnetic reprogrammable coding-metasurface holograms," *Nature Commun.*, vol. 8, p. 197, Aug. 2017.
- [6] Q. Wu and R. Zhang, "Intelligent reflecting surface enhanced wireless network via joint active and passive beamforming," *IEEE Trans. Wirel. Commun.*, vol. 18, pp. 5394–5409, Nov. 2019.
- [7] C. Huang, A. Zappone, G. C. Alexandropoulos, M. Debbah, and C. Yuen, "Reconfigurable intelligent surfaces for energy efficiency in wireless communication," *IEEE Trans. Wirel. Commun.*, vol. 18, pp. 4157–4170, Aug. 2019.
- [8] C. Huang, G. C. Alexandropoulos, A. Zappone, M. Debbah, and C. Yuen, "Energy efficient multi-user MISO communication using low resolution large intelligent surfaces," in *Wkshps. IEEE Globecom*, pp. 1–6, Dec. 2018.
- [9] S. Zargari, A. Khalili, and R. Zhang, "Energy efficiency maximization via joint active and passive beamforming design for multiuser MISO IRS-aided SWIPT," *IEEE Wirel. Commun. Lett.*, vol. 10, no. 3, pp. 557–561, 2021.
- [10] A. Khalili, S. Zargari, Q. Wu, D. W. K. Ng, and R. Zhang, "Multi-objective resource allocation for IRS-aided SWIPT," *IEEE Wirel. Commun. Lett.*, vol. 10, no. 6, pp. 1324–1328, 2021.
- [11] M.-M. Zhao, Q. Wu, M.-J. Zhao, and R. Zhang, "Exploiting amplitude control in intelligent reflecting surface aided wireless communication with imperfect CSI," *IEEE Trans. Commun.*, vol. 69, pp. 4216–4231, Mar. 2021.
- [12] C. You and R. Zhang, "Wireless communication aided by intelligent reflecting surface: Active or passive?," *IEEE Wirel. Commun. Lett.*, vol. 10, pp. 2659–2663, Dec. 2021.
- [13] Z. Zhang, L. Dai, X. Chen, C. Liu, F. Yang, R. Schober, and H. Vincent Poor, "Active RIS vs. passive RIS: Which will prevail in 6G?," Mar. 2021 [Online]. Available: <http://arxiv.org/abs/2103.15154>.
- [14] S. Zeng, H. Zhang, B. Di, Y. Tan, Z. Han, H. V. Poor, and L. Song, "Reconfigurable intelligent surfaces in 6G: Reflective, transmissive, or both?," *IEEE Commun. Lett.*, vol. 25, pp. 2063–2067, Jun. 2021.
- [15] M. H. Khoshafa, T. M. N. Ngatched, M. H. Ahmed, and A. R. Ndjiongue, "Active reconfigurable intelligent surfaces-aided wireless communication system," *IEEE Commun. Lett.*, vol. 25, pp. 3699–3703, Nov. 2021.
- [16] D. Xu, X. Yu, D. W. Kwan Ng, and R. Schober, "Resource allocation for active IRS-assisted multiuser communication systems," in *Proc. IEEE 55th Asilomar Conf. Signals Syst. Comput.*, pp. 113–119, Oct. 2021.
- [17] P. Wang, J. Fang, X. Yuan, Z. Chen, and H. Li, "Intelligent reflecting surface-assisted millimeter wave communications: Joint active and passive precoding design," *IEEE Trans. Veh. Technol.*, vol. 69, no. 12, pp. 14960–14973, 2020.
- [18] D. Zhao, H. Lu, Y. Wang, H. Sun, and Y. Gui, "Joint power allocation and user association optimization for IRS-assisted mmWave systems," *IEEE Trans. Wirel. Commun.*, vol. 21, no. 1, pp. 577–590, 2022.
- [19] A. Alkhateeb, O. El Ayach, G. Leus, and R. W. Heath, "Channel estimation and hybrid precoding for millimeter wave cellular systems," *IEEE J. Sel. Top. Signal Process.*, vol. 8, pp. 831–846, Oct. 2014.
- [20] J.-F. Bousquet, S. Magierowski, and G. G. Messier, "A 4-GHz active scatterer in 130-nm CMOS for phase sweep amplify-and-forward," *IEEE Trans. Circuits Syst. I*, vol. 59, pp. 529–540, Mar. 2012.
- [21] Q. Qi, X. Chen, A. Khalili, C. Zhong, Z. Zhang, and D. W. K. Ng, "Integrating sensing, computing, and communication in 6G wireless networks: Design and optimization," *IEEE Trans. Commun.*, pp. 1–1, 2022.
- [22] J. Jalali, A. Khalili, and H. Steendam, "Antenna selection and resource allocation in downlink MISO OFDMA femtocell networks," in *2020 IEEE 91st Vehicular Technology Conf. (VTC-Spring)*, pp. 1–6, 2020.
- [23] J. Jalali and A. Khalili, "Optimal resource allocation for MC-NOMA in SWIPT-enabled networks," *IEEE Commun. Lett.*, vol. 24, no. 10, pp. 2250–2254, 2020.
- [24] J. Jalali, *Resource allocation for SWIPT in multi-service wireless networks*. M.S. thesis, Dept. Telecommun. Inf. Process., TELIN/IMEC, Ghent Univ., Ghent, Belgium, Jun. 2020.
- [25] S. Bayat, J. Jalali, A. Khalili, M. R. Mili, S. Wittevrongel, and H. Steendam, "Optimal multi-objective resource allocation for D2D underlaying cellular networks in uplink communications," *IEEE Access*, vol. 9, pp. 114153–114166, Jul. 2021.
- [26] A. Rezaei, A. Khalili, J. Jalali, H. Shafiei, and Q. Wu, "Energy-efficient resource allocation and antenna selection for IRS-assisted multicell downlink networks," *IEEE Wirel. Commun. Lett.*, vol. 11, no. 6, pp. 1229–1233, 2022.